IOP Publishing New J. Phys. 25 (2023) 063013 https://doi.org/10.1088/1367-2630/acdc47

New Journal of Physics
The open access journal at the forefront of physics

Deutsche Physikalische Gesellschaft DPG
IOP Institute of Physics

Published in partnership with: Deutsche Physikalische Gesellschaft and the Institute of Physics

OPEN ACCESS

RECEIVED
9 November 2022

REVISED
25 May 2023

ACCEPTED FOR PUBLICATION
7 June 2023

PUBLISHED
16 June 2023

PAPER

Positron acceleration by terahertz wave and electron beam in plasma channel

Zhangli Xu[1], **Baifei Shen**[1,*], **Meiyu Si**[2,3] **and Yongsheng Huang**[2,4]

[1] Department of Physics, Shanghai Normal University, Shanghai 200234, People's Republic of China
[2] Institute of High Energy Physics, Chinese Academy of Sciences, Beijing 100049, People's Republic of China
[3] University of Chinese Academy of Sciences, Beijing 100049, People's Republic of China
[4] School of Science, Shenzhen Campus of Sun Yat-sen University, Shenzhen 518107, People's Republic of China
[*] Author to whom any correspondence should be addressed.

E-mail: bfshen@shnu.edu.cn

Keywords: positron acceleration, intense terahertz wave, coherent transition radiation, particle-in-cell (PIC) simulation

Supplementary material for this article is available online

Abstract

We present a scheme of positron acceleration by intense terahertz (THz) wave together with the driving large-charge electron beam in a plasma channel. The THz wave rapidly evolves into a transversely uniform acceleration field and a weakly focusing/defocusing lateral field in the channel. The THz wave is partially formed with the scheme of coherent transition radiation when the electron beam goes through a metal foil and partially because of the wakefield in the plasma channel. The electron beam continuously supplies energy to the THz wave. Such a field structure offers the feasibility of long-distance positron acceleration while preserving beam quality. By two-dimensional simulations, we demonstrate the acceleration of positrons from initial 1 GeV to 126.8 GeV with a charge of ∼10 pC over a distance of 1 m. The energy spread of accelerated positrons is 2.2%. This scheme can utilize the electron beam either from laser-driven or conventional accelerators, showing prospects towards high-quality and flexible THz-driven relativistic positron sources of ∼100 GeV.

1. Introduction

High-energy positrons are widely distributed in the universe and related to violent high-energy astrophysical phenomena such as pulsar magnetospheres, pair production from black holes and gamma-ray bursts [1, 2]. High-energy gigaelectronvolt (GeV) and even TeV positron beams are crucial for studying these phenomena in laboratories. They also facilitate applications in fundamental nuclear, particle physics, and ultimately, as an indispensable part for realizing electron–positron colliders [3–5], which underpin many significant physical discoveries.

Positrons can be generated via Trident [6, 7], Bethe–Heitler (BH) process [8] and multi-photon Breit–Wheeler process [9]. Currently, the major way of producing positrons in laboratories relies on the BH process, which is based on the collision between energetic electrons with the high-Z atomic fields. Copious positron production has been demonstrated based on either ultraintense laser directly irradiating metallic foils [10, 11] or sending the laser wakefield acceleration electron beams onto high-Z targets [12–14]. Whereas high-energy gain, high-efficiency, and stably beam-loaded electron acceleration has been demonstrated experimentally in the wakefields [15, 16], stable and quality preserving positron acceleration remains a challenge, as the positron beam suffers from defocusing transverse fields. To overcome this issue, drivers including two electron beams [17], hollow electron beam [18, 19], vortex laser [20] and plasmas such as a finite-radius plasma column [21], etc are used to modulate the wakefield structure to accelerate and focus positrons simultaneously.

Another novel and promising positron acceleration scheme relies on coherent transition radiation (CTR) [22], which has recently been experimentally demonstrated in relativistic electron acceleration [23]. Intense

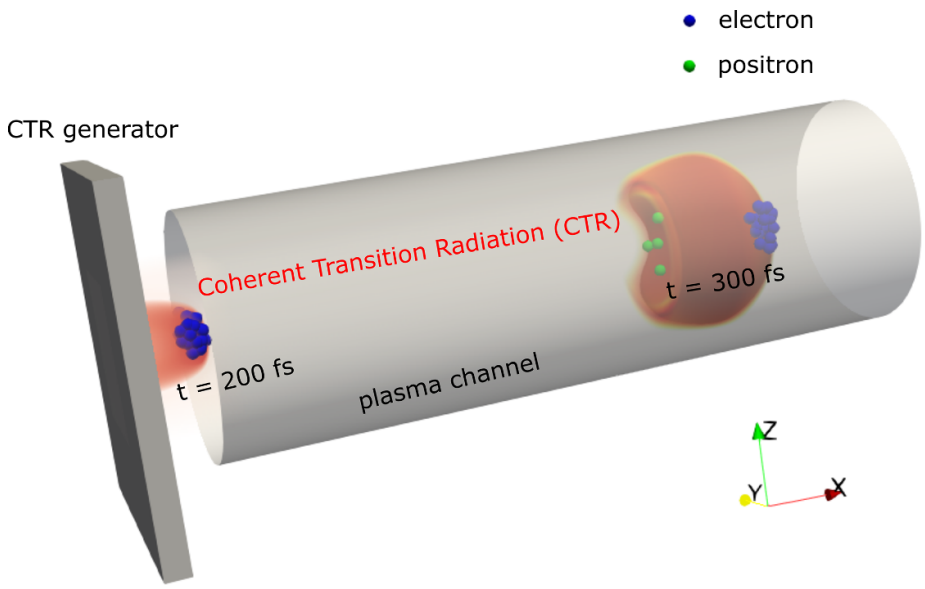

Figure 1. Schematic diagram of quasi-monoenergetic positron acceleration by intense terahertz (THz) wave and electron beam in plasma channel. An electron beam (blue spheres) passing through the interface of two media produces intense THz wave with the scheme of coherent transition radiation (CTR, red isosurface). Then, the THz wave and the electron driver transport in a one-meter-long distance plasma channel, accelerating the injected ∼GeV positrons (green spheres) to ∼100 GeV with narrow energy spread. Red isosurface shows an example of the longitudinal component of THz field at two different times.

CTR generates naturally when the driving electron beam passes through the rear surface of high-Z target, captures and accelerates the generated positrons into high energy. The CTR field resides in terahertz (THz) regime and benefit from the continuously energy supply from the driving electron beam, the CTR field is several orders of magnitude stronger than those involved in conventional THz acceleration scenarios [24–29]. It is different from the mechanisms for THz generation from an embedded plasma dipole [30] or a plasma–vacuum interface [31]. It is a simple and feasible route to utilize positron generation, injection, and acceleration in a single setup. However, the CTR field is spherically divergent in vacuum propagation that it cannot accelerate and confine positrons for a long distance. Thus, it is necessary to find a more practical way to confine or guide the field.

A viable solution is to use hollow plasma channel [32–34]. It is attractive because of its inside vanishing transverse focusing/defocusing fields if the channel is well designed, which ensures emittance preservation of accelerated particles. It has been experimentally demonstrated at FACET in Stanford Linear Accelerator Center (SLAC) to generate an 8 cm long hollow channel and provide gradients of 230 MV m^{-1} to accelerate positrons [35]. Unfortunately, beam breakup (BBU) instabilities in hollow channel [36, 37] greatly destroys the driver and results in a compromised energy conversion efficiency. Near-hollow channels [38] and a coaxial plasma filament [39] can suppress BBU instabilities. Very recently, asymmetric electron driver in hollow plasma channel [40] and a bi-Gaussian density profile electron beam [41] were proposed to excite stable wakefields or a thin hollow filament suitable for positron acceleration. Despite these advances, there is no report of positrons that have been accelerated to ∼100 GeV with narrow energy spread.

In this paper, we present a new scheme of positron acceleration by intense THz wave together with the driving large-charge electron beam in a plasma channel. The basic configuration is sketched in figure 1. Copious energetic electrons pass through a solid target (the CTR generator), as discussed in our previous work [22], and induce intense THz radiation in the plasma channel. The THz wave evolves rapidly in plasma channel to form a steady and uniform field structure, which is suitable for keeping positron acceleration in high quality. Electron driver continuously supply energy to the THz wave when the wave propagates in the channel, and then continuously transfer their energy to positrons. In this way, the positron beam can be accelerated to ∼100 GeV within a distance of only about 1 m.

2. Particle-in-cell simulations

The proposed scheme is confirmed by two-dimensional (2D) particle-in-cell simulations using the EPOCH [42] code. The initial energy of the driving electron bunch is 45 GeV, with a 26.6 nC beam charge. A comparable bunch energy of 42 GeV is utilized in the SLAC [43]. The beam is characterized by a super-Gaussian density profile in both longitudinal and transverse direction,

$n_e = n_{e0}\exp\left(-(x - x_0)^4 \Big/ \delta_{ex}^4 - y^4 \Big/ \delta_{ey}^4\right)$, where $n_{e0} = 1.15 \times 10^{19}$ cm^{-3}, $\delta_{ex} = 3.18$ μm ($\delta_{FWHM} = 5.3$ μm), $\delta_{ey} = 30$ μm ($\delta_{FWHM} = 50$ μm) and $x_0 = 10$ μm, respectively. The CTR generator is modeled by Cu^{1+} ion-electron plasma target, whose density is $n_{Cu} = 8.49 \times 10^{22}$ cm^{-3} and covers the region of $0 < x < 20$ μm. The target fills the simulation window in the transverse direction. The consistence of simulation and theoretical results [22] confirmed that the CTR field induced by the target is the same as that induced by an infinite target. In real experiment, one can always utilize a transversal large enough target to avoid the influence of finite transverse size [44, 45]. We focus on the acceleration process and employ witness positrons to characterize the acceleration effect. The witness positron has an initial energy of 1 GeV and a beam charge of 290 pC, with similar super-Gaussian profiles of $\delta_{px} = 0.8$ μm ($\delta_{FWHM} = 1.33$ μm) and $\delta_{py} = 30$ μm ($\delta_{FWHM} = 50$ μm). Its density, $n_{p0} = 5 \times 10^{17}$ cm^{-3}, is about two orders of magnitude lower than the driving electrons. The center of the positron beam is initially placed 4 μm behind the driving beam, which is optimized for high energy gain and narrow energy spread. One possible way to achieve this configuration is to use two driving electron beams, the first one to induce acceleration field and the second to produce positrons via BH process. Besides, this scheme is promising to be used in conventional accelerators where positrons can be precisely injected into the accelerating phase by external injection. Specific methods need to be investigated further. The initial energy spread, angular distribution and the normalized emittances of the electrons and positrons are neglected. The annihilation of positrons is negligible during the co-propagating process since the lifetime of a positron is expressed as $\tau = 1/\left(\pi r_{e0}^2 c n_{e^-}\right)$, where $r_{e0} \approx 2.82$ fm is the electron classical radius, n_{e^-} is the electron density where positrons are located. In our case, positrons are able to propagate several kilometers without apparent annihilation.

The outer-radius of the plasma channel is $r_0 = 90$ μm and the thickness of the channel wall is 7 μm. At the innermost region ($r < 60$ μm), there is filled rarefied gas with density lower than 10^{15} cm^{-3}. From $r = 60$ μm to the inner-radius of the channel wall, the gas density exponentially increases to 8.49×10^{22} cm^{-3}, a same density as the CTR generator. A moving simulation window of 40 μm (x) $\times$ 180 μm (y) is used and sampled by 400 (x) $\times$ 900 (y) cells. There are five pseudoparticles per cell (PPC) for the driving electron bunch and the witness positrons, and one PPC for the other species. A higher-order particle shape function is applied to suppress numerical self-heating [42].

3. Field structures and results of positron acceleration

In figure 2 we present the evolution of the positron density and the intense THz field in the plasma channel. When initially produced at the rear surface of the CTR generator, the energy of the THz wave is about 0.68 J, accounting for 0.057% of the driving electron beam. The longitudinal component E_x is a single half-cycle positive accelerating field for positrons, with a spherical phase front. In the plasma channel, the field is reflected by the channel walls and exhibits an oscillating electric structure. Due to constant reflection, it becomes uniform and smooth quickly after 100 mm. The longitudinal feature length of the acceleration region is about 22 μm. After that, the accelerating field keeps the relative stable mode and propagates in the plasma channel till to 1 m long, as shown in figure 2(b). Positrons are accelerated in such a transversely uniform region, and are always kept in the accelerating phase ($E_x > 0$) throughout the entire 1 m long distance, as shown in figure 2.

It is worth noting that both CTR and wakefield driven by the electron bunch contribute to the positron acceleration process. In the early stage, the THz wave produced by CTR is vital for trapping and initial acceleration of positrons (see supplementary material for detail). As electrons propagating in the channel, its transverse self-consistent field and the CTR drive electrons in the channel (from both the filled rarefied gas and the channel's inner-wall) to oscillate and form wakefield radiation. The CTR and wakefield are both being reflected by the channel walls and evolves continually to form a relatively flat longitudinal field, which is beneficial for positron acceleration.

Besides the acceleration field, the focusing/defocusing field E_y-cB_z is another critical factor that affects the quality of the positron beam. In the early stage of acceleration process (<100 mm), the positrons are alternately located in the focusing/defocusing field and those undergo strong defocusing field are lost during this process, with a remaining charge of about 50 pC at 100 mm. Then, similar with the E_x field, the focusing/defocusing field consecutively reflected by the channel wall tends to vanish. The positron beam becomes stable without a significant increase in transverse size henceforth.

At about 200 mm, the longitudinal field is fairly homogeneous along the transverse direction and the transverse field E_y-cB_z further vanishes, which is about 1–2 magnitude smaller than the longitudinal field. The positrons are located in weakly focusing/defocusing region and preserve their qualities in the rest long-distance acceleration process. At 1 m, the positron beam remains high density of $\sim 1 \times 10^{16}$ cm^{-3} and

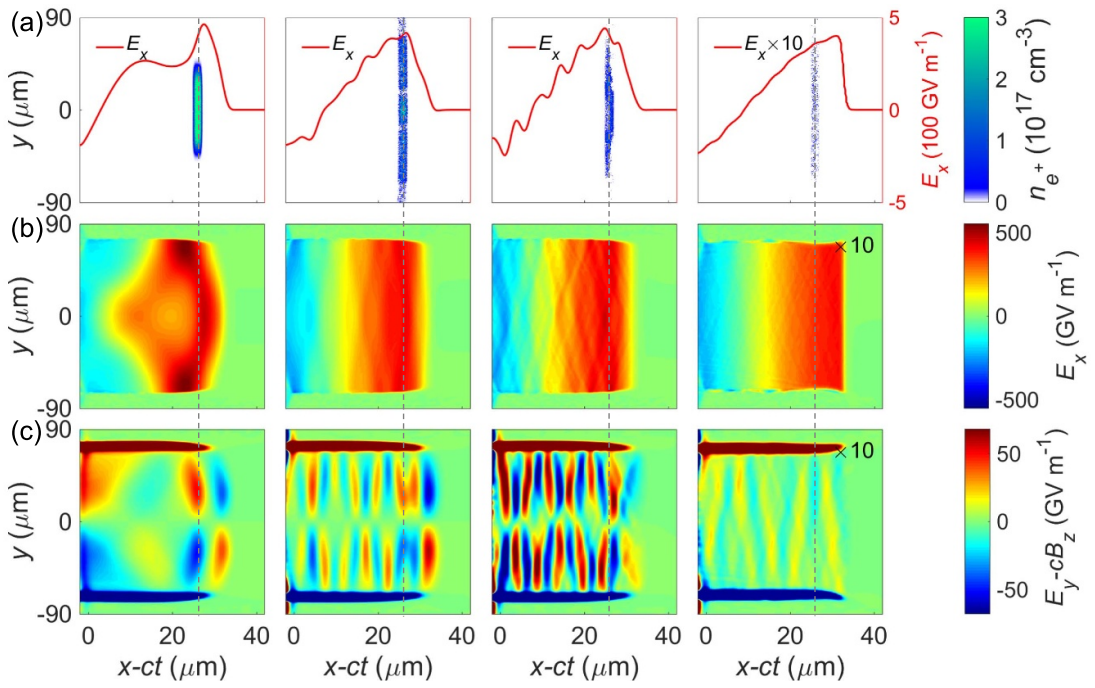

Figure 2. Evolution of positron's density and the THz field in plasma channel. (a) Positron's density, (b) two-dimensional longitudinal E_x and (c) transverse field E_y-cB_z at 0.5, 10, 100, 1000 mm from left to right, respectively. The red solid line in (a) represents the on-axis E_x field. The fields at 1000 mm (the 4th column) is multiplied by ten times.

the normalized transverse emittance is 29 mm mrad. The divergence angle is 0.05 mrad. The acceleration gradient of the field is 40 GV m^{-1} at 1 m that can accelerate positrons even further.

To demonstrate the acceleration results, in figure 3(a) we plot the energy density distribution and the energy spectra of positrons during the acceleration process, $\xi = x\text{-}ct$ is the positron-following coordinate. The energy of positrons increases from initial 1 GeV to 41.8 GeV at 100 mm, with an energy spread of 5.2%. The positrons get continuous quasi-linearly acceleration in the first half of the acceleration process, acquiring the beam energy of 102.2 GeV at 500 mm. The relative energy spread at this momentum is about 2.4%. After that, the energy of the driving electron beam depletes and the acceleration of positrons slows down. At the end of the acceleration, the energy of the positrons finally reaches 126.8 GeV with a lower energy spread of 2.2%. Accelerated positron charge is about 10 pC. The black line in figure 3(b) shows the complete energy acquisition process of the positrons. As we discussed in figures 2(b) and (c), the longitudinal field E_x is uniform in the lateral direction, and the positrons obtain a uniform and stable acceleration. As a result, the absolute energy spread is ∼2.8 GeV at 100 mm, then keeps constant hereafter, shown by the red line in figure 3(b), leading to the continuously decreasing of the relative energy spread. This is benefit from the short pulse of positrons comparing to the length of the THz acceleration region, so the chirp of the field in the x direction has little effect to the absolute energy spread. In addition, the continuous charge loss experienced by the positrons also contribute to the constant energy spread. Considering the remaining acceleration gradient of 40 GV m^{-1} at 1 m, it is expected that smaller relative energy spread could be obtained via our proposed scheme.

During the whole process, the driving electron beam continuously replenishes its own energy to the THz field, which further transfers to positrons. As a consequence, the driven electron beam loses its energy, as shown by the blue line in figure 3(b). At 1 m, the average energy of electrons is 21.7 GeV (maximum energy is 45 GeV) with 100% energy spread.

Moreover, by varying the channel radius and the background plasma density, it is found that such monoenergetic acceleration is robust for certain parameter ranges. This is supported by simulations with different channel profiles (I, II and III), as shown in figure 4(a). The density at innermost region ($r < 60$ μm) of the profiles is ∼10^{13} cm^{-3}, about two orders smaller than that in main simulation. So that profile I is steeper, while profile III, on the contrary, is flatter due to a wider outer-radius of 150 μm. As for channel II, the boundary electron density is ∼10^{18} cm^{-3}, which can be readily achieved by gases. Other electron and positron parameters remained the same. The uniform state of the accelerating fields are achieved in all three cases while positrons obtain energy of more than 100 GeV with monoenergetic peaks, as shown in figure 4(b). The scheme can also work in a lower energy region. By using a driving electron beam with energy

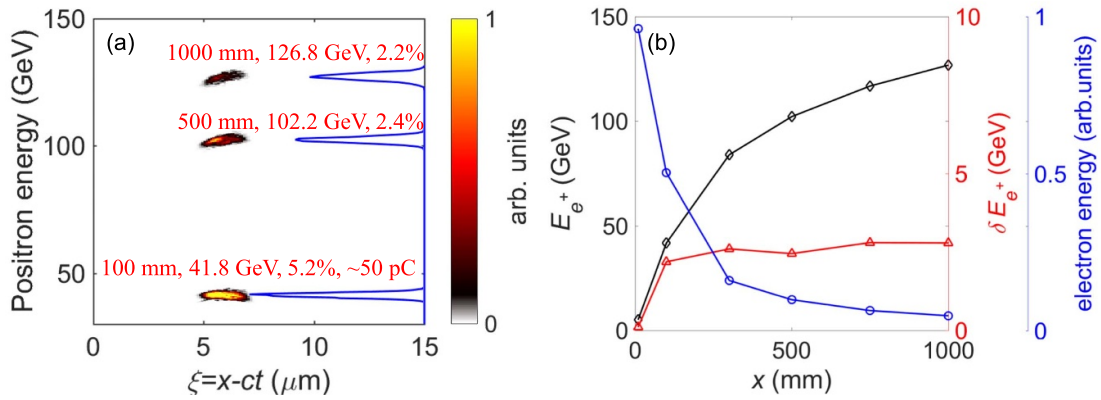

Figure 3. Acceleration results of proposed scheme. (a) Energy spectra and energy–density distributions of positron beam at 100, 500, 1000 mm. (b) Evolution of the energy (black line), energy spread (red line) of the positron beam and the energy of the driving electron beam (blue line).

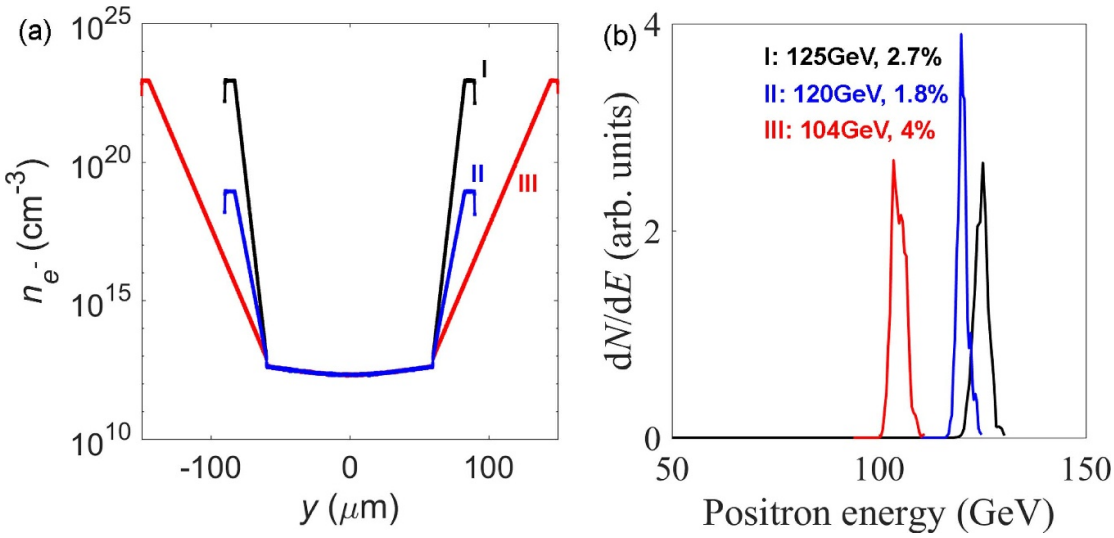

Figure 4. Positron acceleration in different channel. (a) Lateral density distribution of channel profile I, II, and III. (b) Energy spectrum of the positron beam at 970 mm.

of 4.5 GeV and initial witness positron beam of 0.1 GeV, we obtained a high quality quasi-monoenergetic positron beam with peak energy of 15.1 GeV and energy spread of 5.3% after 200 mm. The acceleration gradient at this moment still has 20 GV m^{-1}, which can further accelerate positrons to higher energy.

4. Discussion and conclusion

As a comparison, we perform simulations of positron acceleration without plasma channel. The initial center of the positron beam is also optimized to find a proper accelerating phase in these cases. Other parameters are the same with the plasma channel case. The THz wave now is produced only by the CTR mechanism. It propagates forward as a spherical wave in vacuum, as shown by the longitudinal E_x and transverse fields in figures 5(a) and (b). Therefore, its intensity drops quickly with propagation. It shows apparent intensity-preserving effect of the E_x field in the plasma channel and take advantages throughout the acceleration process. At first 100 mm, the accelerating gradient is about 450 GV m^{-1}, two times larger than that in vacuum. At 1 m, the maximum E_x field in vacuum is 8 GV m^{-1}, five times smaller than that in plasma channel, as shown in figure 5(c). Besides, because of the relatively intense transverse electric field, positrons in vacuum case are almost completely dissipated at 1 m. It is thus difficult to maintain long distance acceleration without plasma channel.

From the discussions above, we conclude that the transversally uniform accelerating field E_x and the weakly focusing/defocusing field establishes quickly in the plasma channel, which are the key to obtaining high-quality acceleration of positron beams. The acceleration region is elongated in the plasma channel,

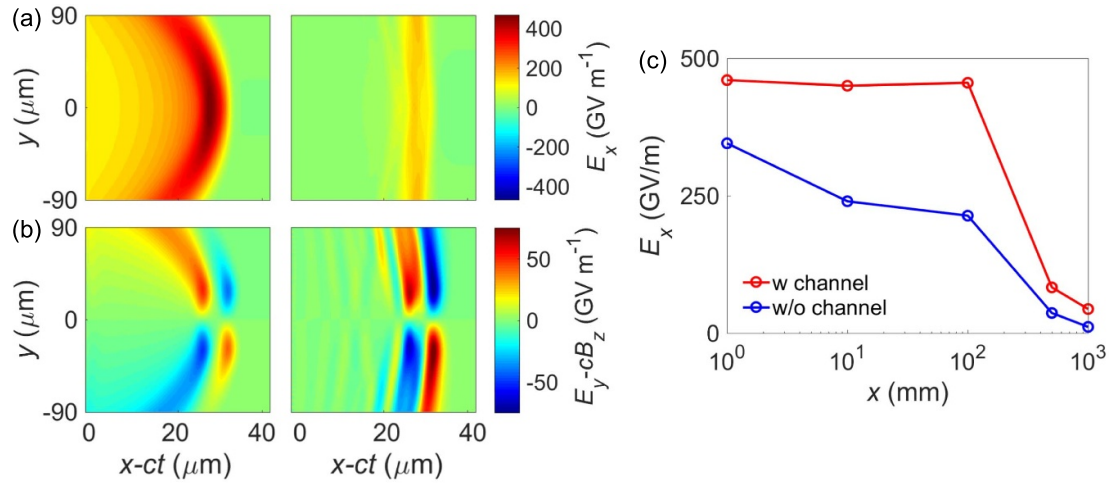

Figure 5. Comparison of THz field in plasma channel and vacuum. (a) Longitudinal E_x and (b) transverse field E_y-cB_z in vacuum at 0.5, 10 mm from left to right. (c) Shows the maximum longitudinal electric field E_x with/without plasma channel.

makes the acceleration field more longitudinal flat, so that positrons are able to find a suitable acceleration phase easier. It shows features of simultaneously maximum energy gain and minimum energy spread if the positron beam being at a proper acceleration phase of the field, which means the acceleration field at this position is intense so that positrons can be quickly captured and survived in strong focusing/defocusing field in the early stage. Also, lateral uniform acceleration field helps to accelerate positrons without obvious increase of energy spread and transverse emittance. Nevertheless, the parameters we selected here are not fully optimized. To get better energy spread of the positron beam, the transversely uniform acceleration field needs to be built up quickly. An elaborate design of the channel, especially the shape of entrance can help to speed up this process. Moreover, one can expect that if the initially injected positron beam is placed close to a steady state, that is, the electron driver has propagated for a while in the channel, a stable acceleration state is built immediately.

In summary, we have demonstrated a novel scheme of long-distance positron acceleration by intense THz wave together with the driving large-charge electron beam in a plasma channel. It relies firstly on the energetic electron bunch to drive intense THz wave through CTR to trap positrons and meanwhile, drive intense wakefield in the channel to accelerate positrons. The electrons continuously supply energy to the THz wave when they propagate in the channel. Then, the plasma channel maintains and modulates the field structure to favor positron acceleration. Our simulation results show that positrons of $\sim$ 10 pC are accelerated from 1 GeV to 126.8 GeV over an accelerated distance of only 1 m, with an energy spread of 2.2%. The emittance is 29 mm mrad with a divergence angel of 0.05 mrad. The obtained results show the promise of using intense THz wave and plasma channel to realize high quality positron acceleration. This scheme can utilize the electron beam either from laser-driven or conventional accelerators, providing a promising way to accelerate high quality positron of $\sim$100 GeV which is vital for future high energy electron–positron colliders.

Data availability statement

The data cannot be made publicly available upon publication because they are not available in a format that is sufficiently accessible or reusable by other researchers. The data that support the findings of this study are available upon reasonable request from the authors.

Acknowledgments

This work was supported by the Ministry of Science and Technology of the People's Republic of China (Grant No. 2018YFA0404803) and the National Natural Science Foundation of China (Grant No. 11935008).

Conflict of interest

The authors declare there are no conflicts of interest related to this work.

ORCID iD

Zhangli Xu https://orcid.org/0000-0002-2456-9299

References

[1] DiPiazza A, Muller C, Hatsagortsyan K Z and Keitel C H 2012 *Rev. Mod. Phys.* **84** 1177–228
[2] Danielson J R, Dubin D H E, Greaves R G and Surko C M 2015 *Rev. Mod. Phys.* **87** 247–306
[3] Shiltsev V D 2012 *Phys.-Usp.* **55** 965–76
[4] Gao J and Jin S 2015 *Chin. Sci. Bull.* **60** 1251–60
[5] Aicheler M, Burrows P, Draper M, Garvey T and Lebrun P 2012 A multi-TeV linear collider based on CLIC technology: CLIC conceptual design report
[6] King B and Ruhl H 2013 *Phys. Rev.*D **88** 013005
[7] Ritus V I 1972 *Nucl. Phys. B* **44** 236–52
[8] Bethe H and Heitler W 1934 *Proc. R. Soc.* A **146** 83–112
[9] Breit G and Wheeler J A 1934 *Phys. Rev.* **46** 1087–91
[10] Chen H *et al* 2010 *Phys. Rev. Lett.* **105** 015003
[11] Chen H, Wilks S C, Bonlie J D, Liang E P, Myatt J, Price D F, Meyerhofer D D and Beiersdorfer P 2009 *Phys. Rev. Lett.* **102** 105001
[12] Sarri G *et al* 2013 *Phys. Rev. Lett.* **110** 255002
[13] Sarri G *et al* 2015 *Nat. Commun.* **6** 6747
[14] Xu T *et al* 2016 *Phys. Plasmas* **23** 033109
[15] Gonsalves A J *et al* 2019 *Phys. Rev. Lett.* **122** 084801
[16] Aniculaesei C *et al* 2022 High-charge 10 GeV electron acceleration in a 10 cm nanoparticle-assisted hybrid wakefield accelerator (arXiv:2207.11492v2)
[17] Wang X, Ischebeck R, Muggli P, Katsouleas T, Joshi C, Mori W B and Hogan M J 2008 *Phys. Rev. Lett.* **101** 124801
[18] Jain N, AntonsenJr T M and Palastro J P 2015 *Phys. Rev. Lett.* **115** 195001
[19] Xu Z Y *et al* 2020 *Phys. Rev. Accel. Beams* **23** 091301
[20] Vieira J and Mendonça J T 2014 *Phys. Rev. Lett.* **112** 215001
[21] Diederichs S, Mehrling T J, Benedetti C, Schroeder C B, Knetsch A, Esarey E and Osterhoff J 2019 *Phys. Rev. Accel. Beams* **22** 081301
[22] Xu Z, Yi L, Shen B, Xu J, Ji L, Xu T, Zhang L, Li S and Xu Z 2020 *Commun. Phys.* **3** 191
[23] Xu H, Yan L, Du Y, Huang W, Tian Q, Li R, Liang Y, Gu S, Shi J and Tang C 2021 *Nat. Photon.* **15** 426–30
[24] Tang H *et al* 2021 *Phys. Rev. Lett.* **127** 074801
[25] Zhang D, Fakhari M, Cankaya H, Calendron A-L, Matlis N H and X K F 2020 *Phys. Rev.* X **10** 011067
[26] Hibberd M T *et al* 2020 *Nat. Photon.* **14** 755–9
[27] Zhang D *et al* 2018 *Nat. Photon.* **12** 336–42
[28] Curry E, Fabbri S, Maxson J, Musumeci P and Gover A 2018 *Phys. Rev. Lett.* **120** 094801
[29] Nanni E A, Huang W R, Hong K H, Ravi K, Fallahi A, Moriena G, Miller R J and Kartner F X 2015 *Nat. Commun.* **6** 8486
[30] Kwon K B, Kang T, Song H S, Kim Y K, Ersfeld B, Jaroszynski D A and Hur M S 2018 *Sci. Rep.* **8** 145
[31] Gupta D N, Jain A, Kulagin V V, Hur M S and Suk H 2022 *Appl. Phys. B* **128** 50
[32] Schroeder C B, Whittum D H and Wurtele J S 1999 *Phys. Rev. Lett.* **82** 1177–80
[33] Chiou T C, Katsouleas T, Decker C, Mori W B, Wurtele J S, Shvets G and Su J J 1995 *Phys. Plasmas* **2** 310–8
[34] Yi L *et al* 2014 *Sci. Rep.* **4** 4171
[35] Gessner S *et al* 2016 *Nat. Commun.* **7** 11785
[36] Lindstrom C A *et al* 2018 *Phys. Rev. Lett.* **120** 124802
[37] Lau Y Y 1989 *Phys. Rev. Lett.* **63** 1141–4
[38] Schroeder C B, Esarey E, Benedetti C and Leemans W P 2013 *Phys. Plasmas* **20** 080701
[39] Pukhov A and Farmer J P 2018 *Phys. Rev. Lett.* **121** 264801
[40] Zhou S, Hua J, An W, Mori W B, Joshi C, Gao J and Lu W 2021 *Phys. Rev. Lett.* **127** 174801
[41] Silva T, Amorim L D, Downer M C, Hogan M J, Yakimenko V, Zgadzaj R and Vieira J 2021 *Phys. Rev. Lett.* **127** 104801
[42] Arber T D *et al* 2015 *Plasma Phys. Control. Fusion* **57** 113001
[43] Blumenfeld I *et al* 2007 *Nature* **445** 741–4
[44] Castellano M, Cianchi A, Orlandi G and Verzilov V A 1999 *Nucl. Instrum. Methods Phys. Res.* A **435** 297–307
[45] Shul'ga N F and Dobrovol'skii S N 1997 *JETP Lett.* **65** 611–4